Design and fabrication of an integrated MEMS-based colloid micropropulsion system

IEPC-2007-099

R. Krpoun[*] , M. Räber[†] and H. R. Shea[‡]
Ecole Polytechnique Fédérale de Lausanne, CH-1015 Lausanne, Switzerland

and

K. L. Smith[§] and J. P. W. Stark[¶]
Queen Mary University of London, London, E1 4NS, United Kingdom

Abstract: The design, microfabrication and initial performance results of a prototype electrospray thruster with integrated individual extractor electrodes are reported in this paper. The aim was to demonstrate increased thrust with an array of emitters spraying simultaneously. Micromachining technologies were employed to achieve large emitter density per surface area, simple integration and good structural repeatability. The novelty of this work lies in the combination of high aspect ratio capillary emitters (height of 70μm, inner diameter of 20μm) with individual extractor electrodes having diameters from 80μm upwards and a spacing as low as 25μm from the capillary tips. The individual integrated electrodes, as opposed to the standard approach of one common electrode, allow for greater uniformity in critical voltages between capillaries and more finely modulated thrust control. Tests with the newly developed thrusters using the ionic liquid EMI-BF$_4$ show that starting voltages below 700V and currents around 300nA per emitter can be achieved.

Nomenclature

d	= distance between emitter tip and extractor plane
E_a	= electrical field at the apex of the cone
m	= mass of the emitted species
p_a	= pressure at the tip of the capillary
q	= charge of the emitted particles
r_a	= radius at the apex of the Taylor cone
R_c	= radius at the tip of the capillary
v_a	= liquid speed at the apex of the cone
V_{cap}	= voltage applied at the capillary emitters
V_{oc}	= critical voltage at which spraying initiates
α	= scaling factor between voltage and electrical field
γ	= surface tension of the liquid used as fuel
ϵ_0	= permittivity of free space
ρ	= density of the liquid

[*]PhD Student, School of Engineering, renato.krpoun@epfl.ch
[†]Master Student, School of Engineering, manuel.raber@epfl.ch
[‡]Assistant Professor, School of Engineering, herbert.shea@epfl.ch
[§]Postdoctoral Research Assistant, Engineering, k.l.smith@qmul.ac.uk
[¶]Professor of Aerospace Engineering, Engineering, j.p.w.stark@qmul.ac.uk

I. Introduction

MICROMACHINING has enabled the downscaling of formerly power, mass and volume consuming systems into small batch-produced low-cost integrated devices. In the wake of this miniaturization, new products have been developed and are commercially available that offer high reliability, low power consumption, low mass and often provide better performance than their predecessors. Microelectromechanical systems (MEMS) are found in many diverse systems such as cars (accelerometers, gyroscopes, pressure sensors), video projectors, mobile telephones, gaming controllers or fiber optic switches. Recent progress in colloid thruster technology, in particular the discovery of an ionic emission mode using the ionic liquid EMI-BF$_4$ as fuel[1], has sparked interest in downscaling this technology to manufacture arrays of capillary emitters with large emitter density per surface area while keeping good structural repeatability and allowing simple system integration.

Prior work on microfabricated out-of-plane electrospray emitters without extraction electrodes has been carried out by Schultz[2], Griss[3] and Wang[4]. Pioneering work on integrated capillary devices has been done by Paine[5], unfortunately the low aspect ratio of his capillaries led to fuel leakage and his devices were not functional. Xiong[6] has demonstrated the feasibility of an integrated device with starting voltages at 1400V. One should further mention the work done by Velásquez-García[7] who studied integrated electrospray thrusters using externally wetted cones rather than capillaries.

This paper presents the results of a feasibility study combining high aspect ratio capillary emitters, having a height of 70μm and an inner diameter of 20μm with individual extractor electrodes having diameters from 80μm upwards and a spacing as low as 25μm from the capillary tips.

II. Thruster Design

The considerations that led to the design of the thrusters were based on results reported in literature, constraints imposed by the microfabrication process and specifications for missions such as LISA or Darwin. The final prototype design features a thruster on a 1cm^2 surface. Fig. 1 shows a schematic cross-section of the experimental assembly. The thruster itself consists of micromachined capillary emitters and extractor electrodes. These chips are assembled on a printed circuit board that provides mechanical support and the necessary electrical interfaces for testing.

A. Performance Estimation

Capillaries were chosen as an alternative to externally wetted tips[7] as it is easier to confine the liquid inside them and thus prevent surface wetting and short-circuits between the extractors and the emitters. For EMI-BF$_4$ Romero-Sanz[1] has observed a beam composed principally of monomers, dimers and trimers for a single capillary emitters with diameters of 20 or 40μm. A current around 300nA can be expected for this tip size. Based on this data a process flow was chosen capable to reproduce capillary arrays with similar dimensions.

The starting voltage was estimated by solving the Laplace equation for a hyperboloid surface acting as
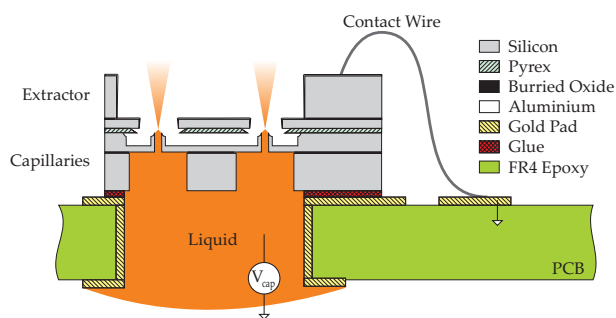

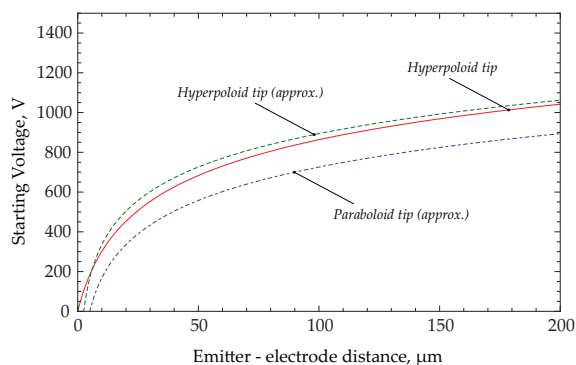**Figure 1. Schematic cross-section of the experimental assembly.**

Figure 2. Estimated starting voltage for a hyperboloid tip model and a parabolic tip model.

the emitter and a flat counter electrode in the prolate-spheroidal coordinate system

$$V_{oc} = \sqrt{\frac{\gamma R_c}{\epsilon_0}} \cdot \frac{\ln\left[\frac{R_c + 2d + 2\sqrt{d(d+R_c)}}{R_c}\right]}{\sqrt{1 + \frac{R_c}{d}}} \tag{1}$$

where γ is the surface tension of the liquid, R_c is the inner diameter of the capillary, ϵ_0 is the permittivity of free space and d the distance between the tip of the hyperboloid and the electrode. A simplified form where $d \gg R_c$ is the expression[9]

$$V_{oc} \cong \sqrt{\frac{\gamma R_c}{\epsilon_0}} \cdot \ln\left[\frac{4d}{R_c}\right]. \tag{2}$$

A similar expression is found if a paraboloidal emitter surface is chosen[10]

$$V_{oc} \cong \sqrt{\frac{\gamma R_c}{\epsilon_0}} \cdot \ln\left[\frac{2d}{R_c}\right]. \tag{3}$$

Fig. 2 shows the results obtained when equations 1,2 and 3 are computed in function of the emitter-electrode distance.

The device has been laid out to pump the fuel passively by capillary effects. To our knowledge all current-voltage models for electrosprays require the knowledge of the liquid flow rate. Therefore a simple model to estimate the voltage versus current characteristics using Bernoulli's principle was developed. This model, presented hereafter, relies on the same basic ideas proposed by Mair[11] and Bell[12], but does not take space charge into account.

The pressure, p_a, at the apex of the cone is

$$p_a = -\frac{1}{2}\epsilon_0 E_a^2 + 2\frac{\gamma}{r_a} \tag{4}$$

where E_a is the electrical field at the apex and r_a the radius of curvature at the apex. At the apex the speed of the liquid, before electrostatic acceleration, with density ρ, charge q and mass m, of either droplets or ions, can be expressed as

$$v_a = \frac{I}{\pi r_a^2 \rho(q/m)}. \tag{5}$$

By assuming that the fluid is ideal (inviscid, incompressible) and that the pressure and speed at the base of the cone are zero the application of Bernoulli's principle yields the expression

$$p_a + \frac{1}{2}\rho v_a = 0. \tag{6}$$

Combining 6 with equations 4, 5 and solving for the current results in

$$I = \pi r_a^2 (q/m)\sqrt{2\rho\left[\left(\frac{1}{2}\epsilon_0 E_a^2\right) - \left(\frac{2\gamma}{r_a}\right)\right]}. \tag{7}$$

The field E_a as a function of voltage at the tip of the apex can be calculated using finite element methods, the obtained results correspond quite well with the measurements as will be shown later.

B.   Geometry and Wafer Layout

A micromachining process flow yielding a suitable geometry for single capillary emitters was identified in the literature[3] and modified to yield large, homogeneous arrays of capillaries on a single wafer. The extractor was inspired by the work done by Corman[8] who suggested the use of a silicon wafer as mask for wet etching a Pyrex wafer. Two designs were developed, one allowing to control each capillary individually and a second, simpler one, where all capillaries emit at the same time. For the laboratory prototype a 4" wafer was segmented into square chips of $1 \times 1\text{cm}^2$ with a thruster layout on each. Fig. 3 shows the basic capillary design where all capillaries have a height of 70μm and are spaced 250μm from each other. Different designs were fabricated, varying the extractor and capillary diameters on the spacing of the emitter from the extractor. An example of capillaries with various diameters is shown in fig. 4.
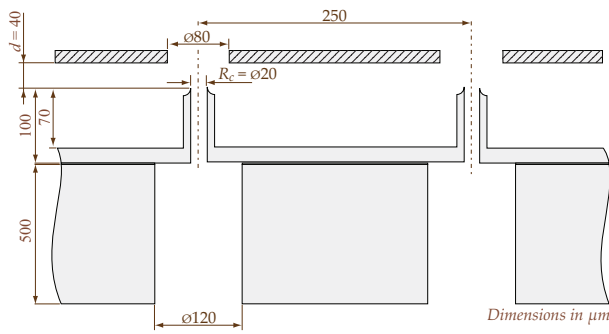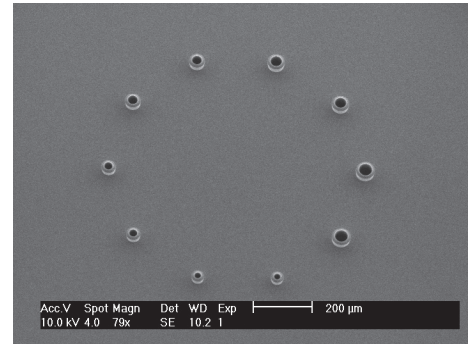
Figure 3. Geometry of the capillaries.

Figure 4. SEM image of a capillary array with varying capillary diameters.

C. Materials

To satisfy long term vacuum and thermal stability the chosen materials have been doped silicon for conducting elements and Borofloat, a borosilicate glass, as electrical insulator. Their combination is an excellent match as they can be joined by clamping the substrates between electrodes, heating them up to 400°C and applying a DC potential of 800V. Under these conditions the sodium ions in the glass are displaced and their depletion leads to a reactive surface that is capable of creating a durable chemical bond with the crystalline silicon wafer. This process, called anodic bonding, is therefore well adapted for spacecraft applications as the use of glue can be avoided. Aluminum is deposited to provide a good contact between the silicon and electrical interfaces on the printed circuit board.

III. Microfabrication

A. Capillary Emitter

The process flow is illustrated in fig. 20. Manufacturing starts by thermal oxidation of a silicon-on-insulator (SOI) wafer. After patterning the oxide (*i*) which will define the stand-off structures, a nitride and oxide layer are deposited and patterned through a second photolithographic step (*ii*). The tip radius is defined by the subsequent isotropic reactive ion etch (RIE), followed by an anisotropic etch (*iii*), called deep reactive ion etching (DRIE). This yields the characteristic outer shape of the capillary. Once the topmost oxide and photoresist layers are removed the wafer is reoxidized at high temperature (*iv*). The nitride is removed and another DRIE performed using the thermal oxidation layer as mask (*v*). Finally the backside is patterned and etched, the buried oxide removed by HF vapor etching and the wafer reoxidized to improve wetting (*vi*).
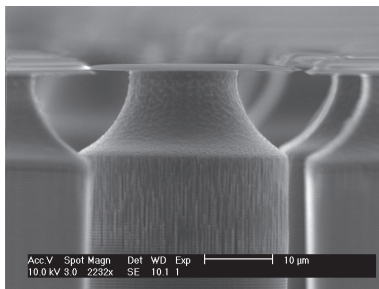

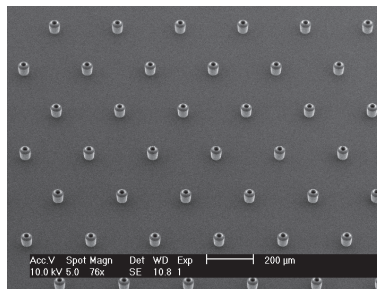Figure 5. Detail of the capillary tip after anisotropic plasma etch. The photoresist, oxide and nitride are still visible.

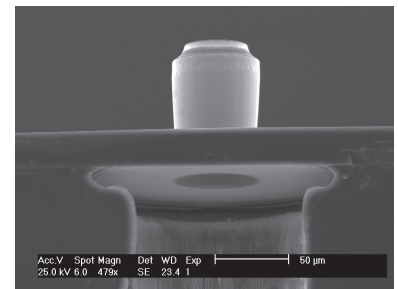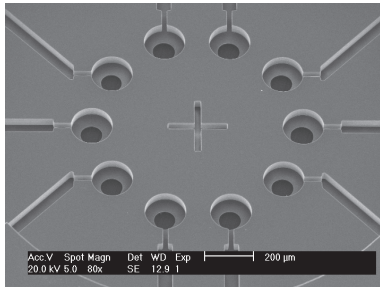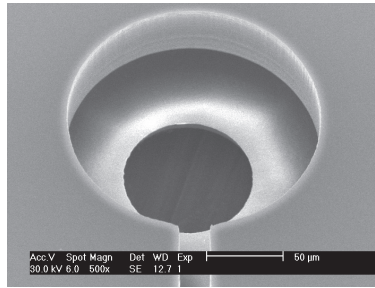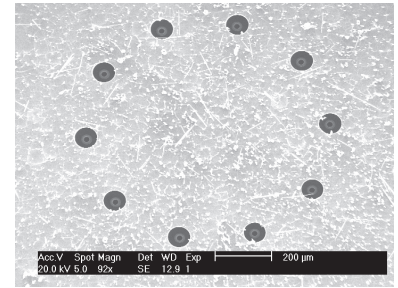Figure 6. SEM image of a large capillary array.

Figure 7. Cut through a capillary wafer, notching is clearly visible below the buried oxide.

Figure 8. Individually addressable capillary emitters.

Figure 9. Detail of an individually addressable capillary emitter.

Figure 10. Image of an assembly of capillary emitters with non-addressable electrodes.

B. Extractor Electrodes

Two process flows were developed to manufacture the extractor electrode. The first design allows to operate all the extractor electrodes simultaneously whereas in the second design the capillary emitters may be operated individually by addressing isolated extractor electrodes. The necessary microfabrication steps are summarized in fig. 21. Both designs start by defining the silicon electrodes through an anisotropic plasma etch on a SOI wafer (1). In a second step a Borofloat wafer is joined by anodic bonding and thinned in a 20% HF solution. For individually adressable extraction electrodes an additional step is needed. First a layer of amorphous silicon is deposited onto the borofloat wafer and patterned. It serves as mask for the anisotropic plasma etch (2b). The backside of both wafers is machined (2a)(3b) and the Borofloat is etched in a 20%HF solution using the pyrex as a mask. Finally a thin layer of aluminium is deposited (3a)(4b) to improve the electrical connection and define the electrodes on the individually adressable arrays.

C. Assembly

The critical part in the assembly of the thruster is the alignment between the extractor electrodes and the capillary emitters. For the first prototype both parts are glued together, chip-wise, under a microscope using a 2-axis translation and rotation stage. This assembly method was satisfactory for initial tests however it will be replaced by anodic bonding at wafer level in the long term. An example of an assembled truster is shown in fig. 10.

IV. Experimental Details

The thruster assemblies were filled with the ionic liquid EMI-BF$_4$ at ambient pressure, mounted onto a support structure (fig. 12) and inserted into a vacuum chamber. The vacuum chamber was equipped with a turbomolecular pump (Varian Turbo-V 551, 550l/s) directly attached to the chamber through an ISO 160 interface, operating pressure during testing was below 1×10^{-5}mbar. The emitter capillaries were connected to a high voltage source (Stanford Research Systems – PS350, ±5kV) and operated at positive or negative voltages. The extractor electrodes were grounded. The electrospray current was measured by means of a Faraday cup (Kimball Physics – FC-72A) attached to a picoammeter (Keithley 487). A grid placed in front of the Faraday cup was biased to a low voltage to capture secondary electrons. To analyze the energy spread of the beam a retarding potential grid was placed in the flight path of the particles. The ionic liquid EMI-BF$_4$ used as fuel was stored in dry conditions to avoid contamination due to water absorption.

V. Results

The tests were carried out using the test facilities described above. To avoid an imbalace in the concentrations of either cations or anions the polarity was reversed periodically. The tests described in the first two subsections were done with chip assemblies where all the extractor electrodes were addressed simultaneously.
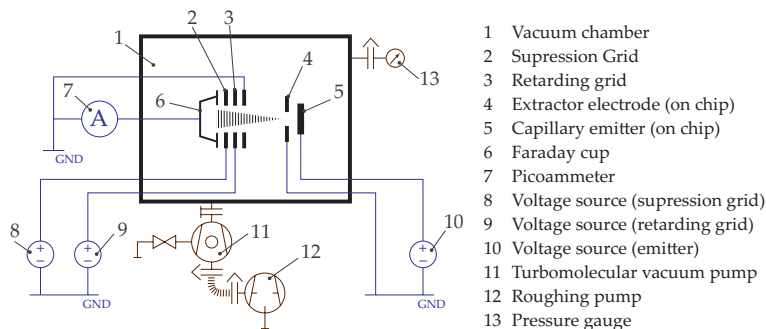
Figure 11. Schematic of the electrospray test rig.

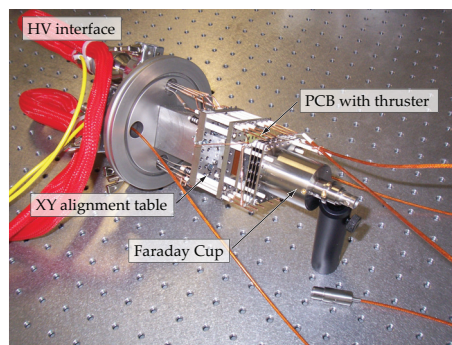|	
1	Vacuum chamber
2	Supression Grid
3	Retarding grid
4	Extractor electrode (on chip)
5	Capillary emitter (on chip)
6	Faraday cup
7	Picoammeter
8	Voltage source (supression grid)
9	Voltage source (retarding grid)
10	Voltage source (emitter)
11	Turbomolecular vacuum pump
12	Roughing pump
13	Pressure gauge

Figure 12. Thruster assembly support structure with mounted Faraday cup.

A. Current vs. voltage characteristics

Measurements were carried out with various thruster configurations. Fig. 13 and 14 show the spraying results of single capillaries with an inner diameter of 20μm and a 140μm diameter electrode. To limit the emission to a single capillary the remaining ones on the chip were blocked by applying a drop of glue on their liquid intake. The spacing between extractor electrodes and the emitter was 25μm for the first measurement and 40μm for the second one. The starting voltage, V_{oc}, can be clearly distinguished from the extinction voltage V_{ox}.

Measurements were also done leaving two capillaries with different extractor diameters open. Fig. 15 shows the obtained results. The emitter with 115μm diameter extractor starts spraying at 700V whereas the one with 140μm starts around 720V. This result shows a way to obtain "discrete" thrust modulation since both sprays are independent from each other.

B. Retarding potential

The beam energy was determined with a retarding potential measurement. Of particular interest was the comparison of the spectra at the starting voltage and the local minimum observed slightly above. Fig. 16 shows the different retarding potential measurements normalized to arbitrary units. Despite the poor resolution of the measurement a clear difference in energy distribution between the starting voltage and subsequent measurements can be seen.
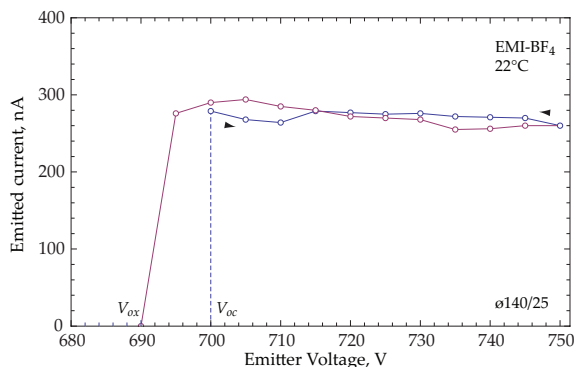

Figure 13. Current-voltage curve for EMI-BF$_4$ of a capillary with 20μm i.d. and a 140μm diameter electrode spaced. 25μm from the emitter

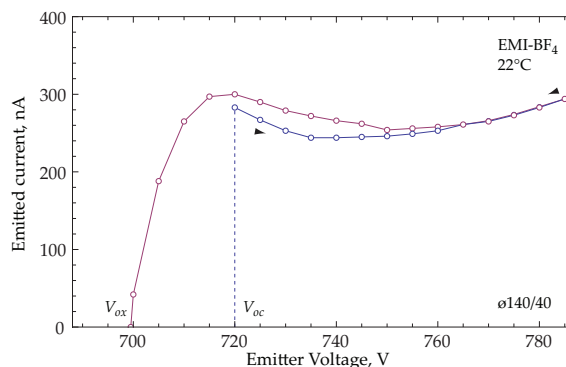**Figure 14. Current-voltage curve for EMI-BF$_4$ of a capillary with 20μm i.d. and a 140μm diameter electrode spaced. 40μm from the emitter**
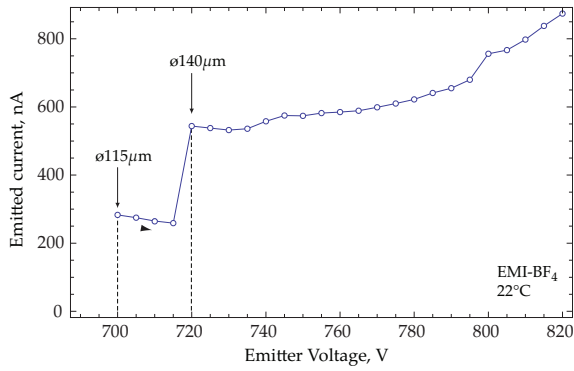
Figure 15. Current-voltage curve for EMI-BF$_4$ of two capillaries with 20μm i.d. with the extraction electrode spaced 40μm from the emitters. The jump in current is due to the different starting voltages of an extractor with 115 and one with 140μm diameter
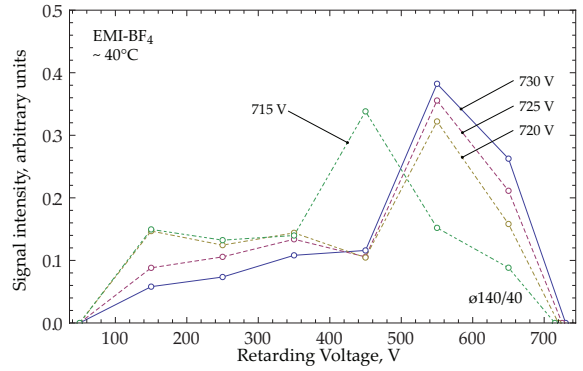

Figure 16. Retarding potential measurement of a capillary with 140μm extractor electrode at 40μm from the emitter. Measurements were taken for different operation voltages

C.   Individually addressable extractor electrodes

A test, with limited success, was carried out with a chip assembly having individually addressable extractor electrodes. Fig. 17 shows such an assembly where each extractor is connected to the printed circuit board through a wire bond. The extractor electrodes from which spraying should not occur were biased to 100V while the spraying one was at ground. The voltage of the capillaries was then gently raised. A fairly stable spray with a current of 150nA starting at 570V was observed, strangely as the voltage was increased by a few volts a large current drop was observed. Unfortunately after some minutes a leakage led to short circuits and the test had to be stopped.

VI.   Discussion

The presented results show the operability of such small thrusters, nevertheless some improvements need to be made to obtain a reliable spray during several thousand hours. In particular wetting and clogging issues are still under investigation. For small extractor holes with a diameter of 80μm the extractor electrodes were clogged and no spray could be observed. For larger diameters liquid droplets were observed around and on top of the extractor (fig. 18). In many cases these liquid spills have been the source of short circuits. While performing measurements shortly after establishing the base pressure variation in the starting voltage
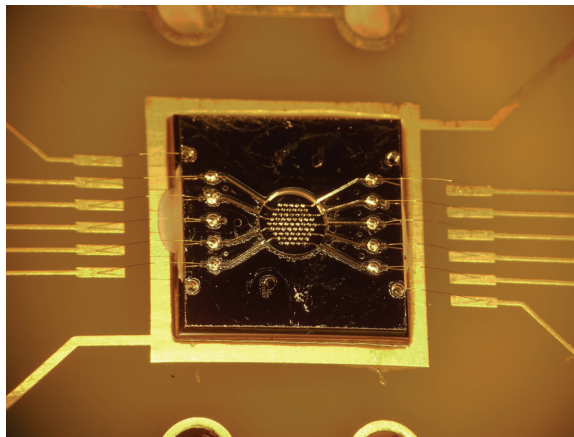

Figure 17. Thruster chip assembly with individually addressable electrodes mounted on a printed circuit board. The electrical contact between chip and PCB is done through wire bonding.

Table 1. Proportionality factor between voltage and electric field based on FEM analysis.

Tip radius, nm	Critical Voltage, V	α – factor, m^{-1}
0.6	745	7.56×10^6
2.8	749	3.56×10^6
12.7	751	1.67×10^6
56.8	748	0.79×10^6
254.5	743	0.39×10^6
1140.6	747	0.18×10^6

where observed. The explanation could be impurities in the liquid that slowly outgas and lead to a change in surface tension, a hypothesis supported by an observed drop in surface tension by 10% when EMI-BF$_4$ is dried[14]. The retarding potential measurements also show a large energy spread in the beam. As argued by Lozano[13] this probably indicates the presence of a jet at the apex of the cone and also the presence of droplets in the beam. Nevertheless time-of-flight measurements need to be performed to give a conclusive answer.

The model used in section II to predict the starting voltage does not provide satisfactory results for this thruster: the critical voltage calculated using eq. 1 yields 465V whereas the measured starting voltage was 710V. This discrepancy could be explained by the fact that the aspect ratio of the capillaries, having a stand-off height of 70μm, is much smaller than a classical electrospray needle leading to a weaker electrical field at the tip of the emitter. If a linear correspondence between the applied voltage and the electrical field at the apex is assumed their relationship can be expressed as

$$E_a = \alpha \times V_{cap} \tag{8}$$

where α is a proportionality factor which depends on the geometry of the capillary and the apex radius. For complex geometries it is determined by finite element modeling. A better way to estimate the starting voltage for a particular geometry can be obtained by introducing expression 8 into equation 7 and solving for zero current

$$V_{oc} = \frac{1}{\alpha}\sqrt{\frac{4\gamma}{\epsilon_0 r_a}}. \tag{9}$$

Table 1 shows the proportionality factor, α, and the critical voltage values computed using a finite element model of the geometry of a capillary with 20μm inner diameter, 140μm extractor diameter spaced by 40μm from the capillary tip. Interestingly the critical voltage seems to be independent of the tip radius once cone
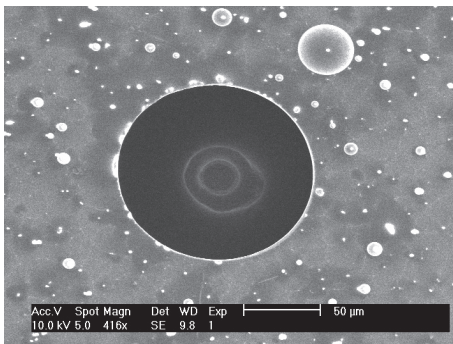
Figure 18. SEM image of droplets observed on top of the extractor electrode. Their provenance could be from the reflected beam during retarding potential measurements.
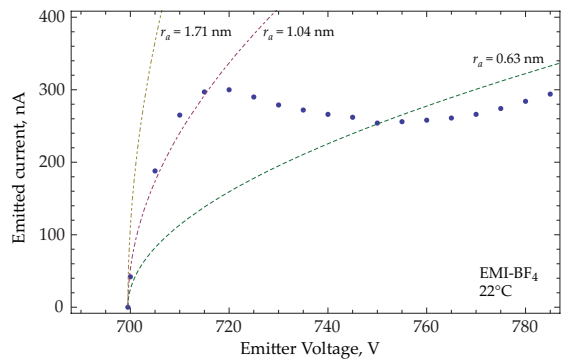
Figure 19. Overlay between a measured current-voltage curve and several calculated ones. The analytical model assumes a purely ionic regime whereas the measured beam contains most likely droplets.

formation has started and the electrical field is no longer distorted by surrounding structures. Although better results are obtained with this approach further measurements need to be done to confirm its validity.

The application of equation 7 to determine the current voltage behavior of the source needs special caution. The difficulties lie in the probable presence of droplets in the beam, the missing information on the apex or jet radius and the absence of viscosity in the model. Nevertheless i-v curves were computed for different apex radii, r_a, using the charge to mass ratio of a simply ionized EMI$^+$ ion. Figure 19 shows an overlay between the measured current (dots), where the voltage was slowly decreased and the computed current-voltage characteristics using the experimentally determined values of α from equation 8. It can be seen that close to the extinction voltage the measured currents lie between the 1.04nm and 1.71nm apex radius curves and diverge for higher voltages.

VII. Conclusion

An electrospray microthruster has been designed, fabricated and tested. The optimized microfabrication process yields large arrays of capillary emitters and extractor electrodes with well defined geometries. The operation of the devices for several geometries has been experimentally demonstrated. Beam currents around 300nA have been measured, the large energy dispersion measured using a retarding potential analyzer indicate the presence of a jet at the apex of the Taylor cone. A simple current-voltage model, based on the Bernoulli principle has been proposed. A first correlation with the obtained results has shown promising results, but further measurements need to be performed to confirm its validity.

Acknowledgments

References

[1]Romero-Sanz, I., Bocanegra, R. and Fernandez de la Mora, J., "Source of Heavy Molecular Ions Based on Taylor Cones of Ionic Liquids Operating in the Pure Ion Evaporation Regime," *Journal of Applied Physics*, Vol. 94, No. 5, 2003, pp. 3599–3605.

[2]Schultz, G. A., Corso, T. N., Prosser, S. J. and Zhang, S.,"A fully integrated monolithic microchip electrospray device for mass spectrometry,"' *Analytical Chemistry*, Vol. 72, 2000, pp. 4058–4063.

[3]Griss, P. and Melin, J. and Sjödahl, J. and Roeraade, J., "Development of Micromachined Hollow Tips for Protein Analysis Based on Nanoelectrospray Ionization Mass Spectrometry," *Journal of Micromechanics and Microengineering*, Vol. 12, 2002, pp. 682–687.

[4]Wang, L., Stevens, R., Malik, A., Rockett, P., Paine, M., Adkin, P., Martyn, S., Smith, K., Stark, J. and Dobson, P., "High-aspect-ratio silica nozzle fabrication for nano-emitter electrospray applications," *Microelectronic Engineering*, Vol. 84, No. 5–8, 2007, pp. 1190–1193.

[5]Paine, M. D.,"A Micro-Fabricated Colloid Microthruster," Ph.D. Dissertation, Department of Aeronautics and Astronautics, University of Southampton, 2002.

[6]Xiong, J., Zhou, Z., Sun, D. and Ye, X.,"Development of a MEMS based colloid thruster with sandwich structure," *Sensors and Actuators A: Physical*, Vol. 117, No. 1, 2005, pp. 168–172.

[7]Velásquez-García, L. F., Akinwande, A. I. and Martínez-Sánchez, M., "A Planar Array of Micro-Fabricated Electrospray Emitters for Thruster Applications," *Journal of Microelectromechanical Systems*, Vol. 15, No. 5, 2006, pp. 1272–1280.

[8]Corman, T. and Enoksson, P. and Stemme, G., "Deep Wet Etching of Borosilicate Glass Using an Anodically Bonded Silicon Substrate as Mask," *Journal of Micromechanics and Microengineering*, Vol. 8, No. 2, 1998, pp. 84–87.

[9]Carretero-Benignos, J. A.,"Numerical Simulation of a Single Emitter Colloid Thruster in Pure Droplet Cone-Jet Mode," Ph.D. Dissertation, Department of Mechanical Engineering, Massachusetts Institute of Technology, 2005.

[10]Prewett, P. D. and Mair, G. L. R., *Focused ion beams from liquid metal ion sources*, Research Studies Press LTD., Taunton, 1991, Chap. 3.

[11]Mair, G. L. R., "Theoretical determination of current-voltage curves for liquid metal ion sources," *Journal of Physics D: Applied Physics*, Vol. 17, No. 11, 1984, pp. 2323–2330.

[12]Bell, A. E. and Swanson, L. W., "Mechanisms of liquid metal ion source operation," *Nuclear instruments and methods in physics research section B: Beam interactions with materials and atoms*, Vol. 10–11, No. 2, 1985, pp. 783–787.

[13]Lozano, P. C., "Energy properties of an EMI-Im ionic liquid ion source," *Journal of Physics D: Applied Physics*, Vol. 39, 2006, pp. 126–134.

[14]Martino, W., Fernandez de la Mora, J., Yoshida, Y., Saito, G. and Wilkes, J., "Surface tension measurements of highly conducting ionic liquids," *Green Chemistry*, Vol. 8, 2006, pp. 390–397.
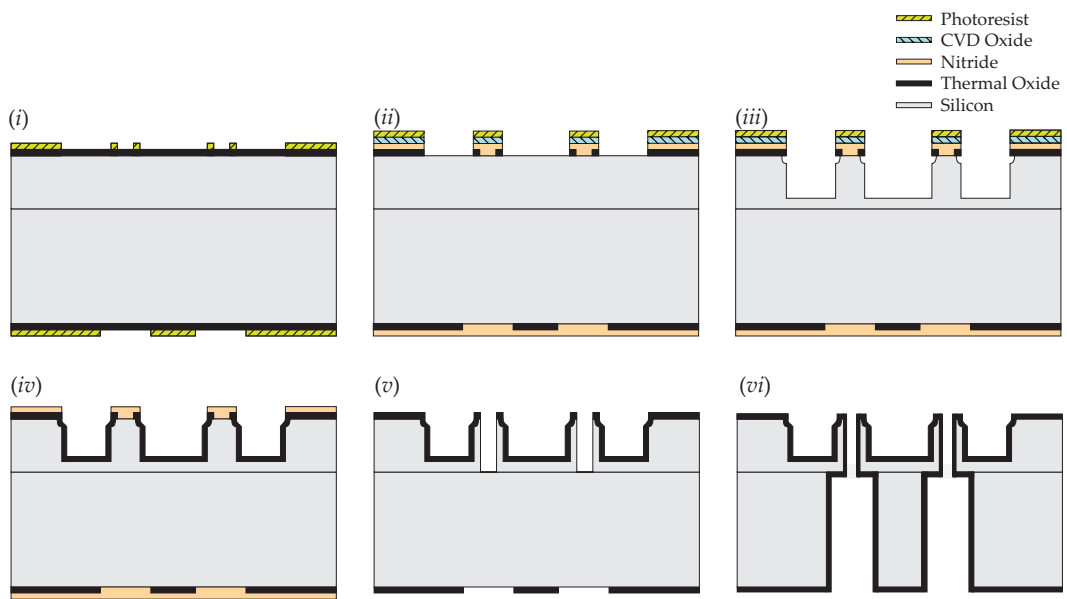
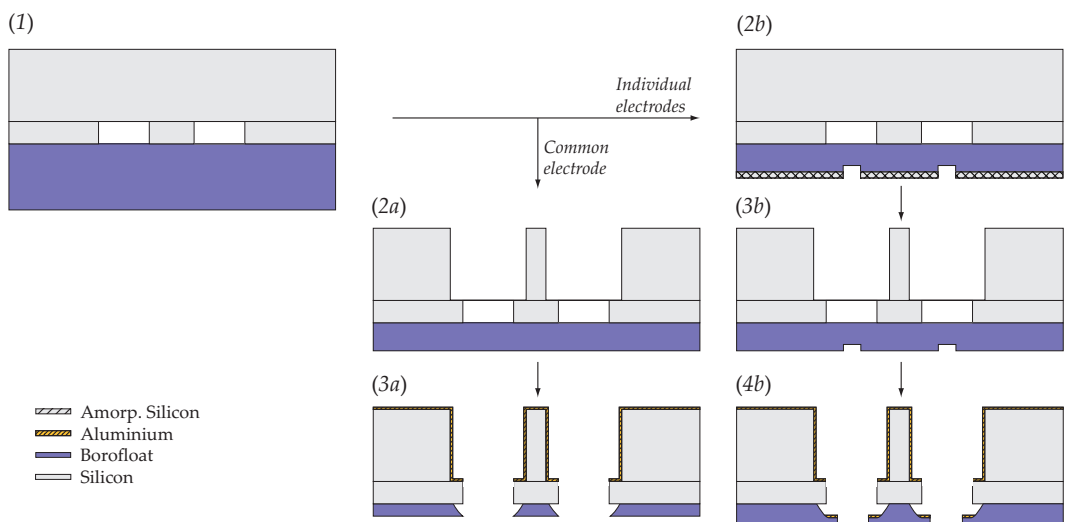**Figure 20. Microfabrication steps of capillary emitter tips.**

Figure 21. Microfabrication steps of extractor electrodes.